*J. Fluid Mech.* (1987), *vol.* 184, *pp.* 581–597
*Printed in Great Britain*



# The initial evolution of gravity–capillary waves

By PETER A. E. M. JANSSEN†
Department of Oceanography, KNMI, De Bilt, The Netherlands

(Received 8 December 1986)

In this paper we discuss the initial evolution of wind-generated, gravity–capillary waves by means of a dynamical model that includes the effects of wind input, viscous dissipation and three-wave interactions. In particular, we study the generation of the initial wavelets by wind and the subsequent migration of the peak of the spectrum to lower wavenumbers. Under certain conditions a sudden migration of the peak wavenumber is found. It is argued that this sudden migration is related to the phenomenon of second-harmonic resonance. We also observe that during the generation of the initial wavelets by wind, nonlinear three-wave interactions may be important. Therefore, the experimental determination of the growth rate of the waves by wind by just analysing the time series of the surface elevation (as is done by e.g. Kawai 1979 and Plant & Wright 1977) might be in error.

## 1. Introduction

In this paper we shall discuss the evolution of wind-generated, gravity–capillary waves, with emphasis on the effect of three-wave interactions. Choi (1977) investigated experimentally the evolution of gravity–capillary waves in the presence of wind. The fetch dependence of the wave variance spectrum was determined and he observed at a certain fetch a rather sudden transition of the peak frequency of the spectrum to half its initial value. This period doubling may also be observed in the spectra obtained by Kawai (1979). Kawai distingusihed between two stages of growth, one where only linear effects due to growth of the wind were thought to be present (the stage of the initial wavelets) and a stage where nonlinear effects become important. Plant & Wright (1977) studied the energy balance of gravity–capillary waves and concluded that resonant three-wave interactions play an important role in the evolution of these waves, while the effect of resonant four-wave interactions is only minor. They did not observe period doubling, presumably because their interest was in later stages of growth.

Chen & Saffman (1979) suggested that the observed period doubling is related to the phenomenon of second-harmonic resonance. Second-harmonic resonance occurs if the frequency of the free wave at wavenumber $2k$ (a free wave is a wave that obeys a dispersion relation $\omega = \omega(k)$) is twice the frequency of the free wave at wavenumber $k$, i.e.

$$\omega(2k) = 2\omega(k). \tag{1}$$

For pure gravity–capillary waves with dispersion relation

$$\omega = (gk + Tk^3)^{\frac{1}{2}}, \tag{2}$$

† Present address ECMWF, Shinfield Park, Reading, UK.

where $g$ is the acceleration due to gravity and $T$ is surface tension, the condition (1) for second-harmonic resonance is satisfied for the wavenumber $k_0$,

$$k_0 = 2k = \left(\frac{2g}{T}\right)^{\frac{1}{2}}. \tag{3}$$

Whenever this conditions is met there is a strong nonlinear interaction between the free wave at wavenumber $k$ and its second harmonic. Simmons (1969) conjectured that when gravity–capillary waves are generated near the second harmonic by wind the effect of second-harmonic resonance is to transfer energy from the second harmonic to the first harmonic.

Janssen (1986) obtained a simple dynamical model for the strong, nonlinear interaction between the first and second harmonic that includes the effects of wind input, viscous dissipation and shear in the water current. Period doubling was found to occur rather suddenly as growth by wind combined with nonlinear interaction gave a bi-exponential growth of the waves at half the initial peak frequency.

Here, we present some (numerical) results of a more general model of the evolution of wind-induced, gravity–capillary waves. Our starting point is a gravity–capillary wave field in isolation. As was shown by Zakharov (1968), such a wave field constitutes a Hamiltonian system and the dynamics of the waves are determined by Hamilton's equations. Zakharov expressed the Hamiltonian in a power series of essentially the wave amplitude. Retaining terms up to third order in wave amplitude, one finds that the rate of change of the wave amplitude in time is determined by three-wave interactions only. According to estimates of Plant & Wright (1977), for gravity–capillary waves the effect of higher-order nonlinearity is quite small. We perturb this Hamiltonian system by including the effects of wind input and viscous dissipation, assuming that nonlinearity and the latter effects are small but equally important.

The objective is to study the initial-value problem that at time $t = 0$ starts with a white-noise spectrum. The wind is then switched on and our interest is in the evolution in time of the wavenumber spectrum and related quantities. Please note that one therefore hopes to expect wavelength doubling instead of the period doubling in experiment. The resulting set of ordinary differential equations is solved by means of a Runge–Kutta 4 integration method. This method appears to be very accurate as is illustrated by the case of a wave field in isolation (hence, no wind input or viscous dissipation) where energy and momentum are conserved up to 7 significant digits for periods of about 50–100 typical wave periods.

First, in order to check on errors, the numerical code was applied to a case that may be treated analytically, namely the special case that only the waves obeying the condition for second-harmonic resonance are present (cf. (1)). The numerical results are in excellent agreement with analytical results as obtained by Janssen (1986), e.g. wind input gives rise to a very sudden transfer of energy from the second harmonic to the first harmonic (wavelength doubling).

Then, we use the numerical code for a one-dimensional simulation of the generation of a spectrum of gravity–capillary waves by wind. We have chosen the number of modes and the mesh width in wavenumber space in such a way that the highest wavenumber is well inside the viscous subrange. In practice this means that we take a spectrum of waves with 25–50 components. We have performed a systematic study of the dependence of the evolution of gravity–capillary waves on the initial noise level (at constant wind speed). In all the cases nonlinear effects due to three-wave interactions affect the evolution of the wave spectrum, although for

small initial noise levels this happens at later stages of wave growth. Nonlinearity gives rise to a down-shift in the peak wavenumber by a factor of two. We have also studied the dependence on wind speed at a constant noise level. In particular, we consider three special cases. The first one has its maximum input of energy just below the wavenumber $k_0$ (cf. (3)) for second-harmonic resonance, whereas the second case has the maximum input of energy at the wavenumber $k_0$. The last case, which most resembles Choi's experiment, has its maximum energy input at a wavenumber slightly above $k_0$. Interestingly, during the stage of the initial wavelets (using Kawai's terminology) a narrow spectral peak is generated, much narrower than one would expect from the linear theory of wind-wave generation alone. It is shown that three-wave interactions give rise to an enhanced growth of the spectral peak. After the stage of the initial wavelets a very sudden downshift of the peak wavenumber is observed. All this is in qualitative agreement with Choi's experiment.

We have chosen a deterministic instead of a statistical approach because apart from the consideration that a statistical theory of an ensemble of wave systems might not give an appropriate description of a laboratory experiment, the conventional statistical theory of three-wave interactions fails in case of second-harmonic resonance (Davidson 1972; Valenzuela & Laing 1972). This immediately follows from the evolution equation for the action density $n$, which reads (Davidson 1972)

$$s_1 \frac{\partial}{\partial t} n_1 = 4\pi \int_{-\infty}^{\infty} \mathrm{d}\boldsymbol{k}_2\, \mathrm{d}\boldsymbol{k}_3\, \delta(\boldsymbol{k}_2+\boldsymbol{k}_3-\boldsymbol{k}_1)\, \delta(\omega_2+\omega_3-\omega_1) |V(-1,2,3)|^2 \times \{s_1 n_2 n_3 - s_2 n_1 n_3 - s_3 n_1 n_2\}, \quad (4)$$

where $n_1 = n(\boldsymbol{k}_1)$, etc, $s_1 = \mathrm{sign}\,(\boldsymbol{k}_1)$, $V(-1,2,3)$ is the interaction coefficient as given by Zakharov, and $\omega_1 = s_1\, \omega(k_1)$ with $\omega$ given by (2). When performing the integrations over $\boldsymbol{k}_2$ and $\boldsymbol{k}_3$, the delta function over the frequencies give rise to a Jacobian $J$ and the rate of change of $n_1$ is proportional to

$$J = \left| \frac{\mathrm{d}}{\mathrm{d}k_2} \omega_2 - \frac{\mathrm{d}}{\mathrm{d}k_3} \omega_3 \right|^{-1}, \quad (5)$$

where $\boldsymbol{k}_2$ and $\boldsymbol{k}_3$ are expressed as functions of $\boldsymbol{k}_1$ by solving the resonance conditions

$$\omega_1 = \omega_2 + \omega_3, \quad \boldsymbol{k}_1 = \boldsymbol{k}_2 + \boldsymbol{k}_3.$$

In the special case of second harmonic resonance $\boldsymbol{k}_2 = \boldsymbol{k}_3 = \frac{1}{2}\boldsymbol{k}_0$ (where for gravity–capillary waves $\boldsymbol{k}_0$ is given by (3)) and the Jacobian becomes infinite, because the group velocities of mode 2 and mode 3 become equal. This means that according to the evolution equation (4) there would be an instant relaxation to a spectrum that obeys the condition that the terms in curly brackets in (4) for the resonant modes in question vanish, or

$$n(k_0) = \tfrac{1}{2} n(\tfrac{1}{2} k_0). \quad (6)$$

Although this might be an appropriate condition if one is interested in long timescales it is certainly not valid for the initial evolution of gravity–capillary waves in a wind-wave tank, where at the start waves are being generated around $k = k_0$. We conclude from this that second-harmonic resonance must play an important role in the evolution of the surface waves. Needless to say in the remainder of this paper we are especially interested in the energy transfer near the second-harmonic wavenumber as obtained from the deterministic equations.

## 2. Evolution equation for gravity–capillary waves

Our starting point is the Hamiltonian for surface waves introduced by Zakharov (1968) (see also Broer 1974; Miles 1977). The total energy of the fluid is (apart from the constant water density $\rho_w$)

$$E = \frac{1}{2}\int \mathrm{d}\boldsymbol{r} \int_{-\infty}^{\eta} \left[ (\nabla\phi)^2 + \left(\frac{\partial}{\partial z}\phi\right)^2 \right] \mathrm{d}z + \tfrac{1}{2}g\int \mathrm{d}\boldsymbol{r}\,\eta^2 + T\int \mathrm{d}\boldsymbol{r}\,[1+(\nabla\eta)^2)^{\frac{1}{2}} - 1]. \tag{7}$$

Here, $\eta$ is the surface elevation, $\phi$ the velocity potential, $g$ the acceleration due to gravity, $T$ the surface tension and $\nabla$ the horizontal gradient.

Choosing as canonical variables the surface elevation $\eta$ and the velocity potential at the surface $\psi = \Phi(z, \boldsymbol{r}, t)|_{z=\eta}$, Hamilton's equations

$$\frac{\partial}{\partial t}\eta = \frac{\delta E}{\delta \psi}, \quad \frac{\partial}{\partial t}\psi = -\frac{\delta E}{\delta \eta} \tag{8}$$

have been shown to be equivalent to the kinematic and pressure condition at the surface. Zakharov proceeded by introducing the Fourier transforms of $\eta$ and $\psi$,

$$n(\boldsymbol{k}) = \frac{1}{2\pi}\int \mathrm{d}\boldsymbol{r}\,\eta(\boldsymbol{r})\,\mathrm{e}^{-\mathrm{i}\boldsymbol{k}\cdot\boldsymbol{r}}, \quad \psi(\boldsymbol{k}) = \frac{1}{2\pi}\int \mathrm{d}\boldsymbol{r}\,\psi(\boldsymbol{r})\,\mathrm{e}^{-\mathrm{i}\boldsymbol{k}\cdot\boldsymbol{r}}, \tag{9}$$

thus solving the boundary-value problem for the potential $\phi$,

$$\Delta\phi = 0 \text{ in the region } \{z | -\infty < z < \eta\}, \tag{10}$$

in an iterative manner. Finally, Zakharov introduced the complex variables $a(\boldsymbol{k})$ and $\mathrm{i}a^*(\boldsymbol{k})$ according to

$$\left.\begin{aligned} \eta(\boldsymbol{k}) &= \frac{1}{\sqrt{2}}\frac{k^{\frac{1}{2}}}{\omega^{\frac{1}{2}}}A(\boldsymbol{k}), \quad A(\boldsymbol{k}) = a(\boldsymbol{k}) + a^*(-\boldsymbol{k}), \\ \psi(k) &= -\frac{\mathrm{i}}{\sqrt{2}}\frac{\omega^{\frac{1}{2}}}{k^{\frac{1}{2}}}B(\boldsymbol{k}), \quad B(\boldsymbol{k}) = a(\boldsymbol{k}) - a^*(-\boldsymbol{k}) \end{aligned}\right\} \tag{11}$$

(where $\omega = (gk + Tk^3)^{\frac{1}{2}}$ and $k = |\boldsymbol{k}|$) in order to be able to express the energy in the form of a series in powers of $a(\boldsymbol{k})$ and $a^*(\boldsymbol{k})$. Hamilton's equations (8) then become the single equation

$$\frac{\partial}{\partial t}a(\boldsymbol{k}) = -\mathrm{i}\frac{\delta E}{\delta a^*(\boldsymbol{k})}. \tag{12}$$

Some simplifcations of the resulting evolution equation may be obtained by the restriction that the waves are only propagating to the right as we are interested in wind-generated surface waves. Also, from now on we shall only consider one-dimensional propagation. To second order in wave amplitude, the evolution equation for the complex amplitude $A$ (cf. (11)) then becomes

$$\frac{\partial}{\partial t}A_1 = -\mathrm{i}s_1\omega_1 A_1 - \mathrm{i}s_1\int_{-\infty}^{\infty} \mathrm{d}\boldsymbol{k}_2\,\mathrm{d}\boldsymbol{k}_3\,\delta(\boldsymbol{k}_2+\boldsymbol{k}_3-\boldsymbol{k}_1)\,V(-1,2,3)\,A_2A_3, \tag{13}$$

where $A_1 = A(\boldsymbol{k}_1)$, $s_1 = \mathrm{sign}\,(\boldsymbol{k}_1)$, $\delta$ is the Dirac delta function and the interaction matrix $V$ is given by (Zakharov 1968; Crawford *et al.* 1981)

$$\begin{aligned} V(1,2,3) = \frac{1}{8\pi\sqrt{2}}\Bigg[ &(\boldsymbol{k}_1\cdot\boldsymbol{k}_2 + k_1k_2)\left\{\frac{\omega_1\omega_2}{\omega_2}\frac{k_3}{k_1k_2}\right\}^{\frac{1}{2}} + (\boldsymbol{k}_1\cdot\boldsymbol{k}_3 + k_1k_3)\left\{\frac{\omega_1\omega_3}{\omega_2}\frac{k_2}{k_1k_3}\right\}^{\frac{1}{2}} \\ &+ (\boldsymbol{k}_2\cdot\boldsymbol{k}_3 + k_2k_3)\left\{\frac{\omega_2\omega_3}{\omega_1}\frac{k_1}{k_2k_3}\right\}^{\frac{1}{2}}\Bigg]. \end{aligned} \tag{14}$$

An alternative form of the evolution equation for $A$ may be obtained by using the property $A^*(-k) = A(k)$, which follows from the reality of the surface elevation. Using this property and some symmetry properties of $V$, an equation for $A_1$, $k_1 > 0$, with positive wavenumber arguments only, may be obtained. The result is

$$\frac{\partial}{\partial t}A_1 = -\mathrm{i}\omega_1 A_1 - \mathrm{i}\int_0^\infty \mathrm{d}\boldsymbol{k}_2\,\mathrm{d}\boldsymbol{k}_3\{\delta(\boldsymbol{k}_1-\boldsymbol{k}_2-\boldsymbol{k}_3)\,V(-1,2,3)\,A_2A_3 + 2\delta(\boldsymbol{k}_1-\boldsymbol{k}_2+\boldsymbol{k}_3)\,V(-1,2,-3)\,A_2A_3^*\}. \quad (15)$$

Equation (15) admits a numbers of conserved quantities. The first is the Hamiltonian $H$, which is however not the total energy of the fluid as (15) is an approximation of (12). The Hamiltonian is given by

$$H = \int_0^\infty \mathrm{d}k_1\,\omega_1|A_1|^2 + \int_0^\infty \mathrm{d}\boldsymbol{k}_1\,\mathrm{d}\boldsymbol{k}_2\,\mathrm{d}\boldsymbol{k}_3\,\delta(\boldsymbol{k}_2+\boldsymbol{k}_3-\boldsymbol{k}_1)\,V(-1,2,3)\{A_1^*A_2A_3 + A_1A_2^*A_3^*\}, \quad (16)$$

and the evolution equation (15) follows from Hamilton's equation

$$\frac{\partial}{\partial t}A_1 = -\mathrm{i}\frac{\delta H}{\delta A_1^*},$$

considering $A_1$ and $\mathrm{i}A_1^*$ as independent canonical variables. It is emphasized that for the deterministic equations the 'energy' is given by the complicated expression for $H$; it involves cubic terms in the wave amplitude.

Another conserved quantity is wave momentum. It is defined by

$$P = \int_0^\infty \mathrm{d}k_1\,k_1|A_1|^2, \quad (17)$$

and $P$ is conserved, as may be checked by calculating $\mathrm{d}P/\mathrm{d}t$ while using the symmetry properties of $V$.

So far we have considered conservative wave–wave interactions. The effects of wind input and viscous dissipation can however simply be included in the case where these physical processes are as important as the three-wave interactions. The final result then is

$$\frac{\partial}{\partial t}A_1 = (-\mathrm{i}\omega_1 s_1 + \gamma_1)A_1 - \mathrm{i}s_1\int_{-\infty}^\infty \mathrm{d}\boldsymbol{k}_2\,\mathrm{d}\boldsymbol{k}_3\,\delta(\boldsymbol{k}_2+\boldsymbol{k}_3-\boldsymbol{k}_1)\,V(-1,2,3)\,A_2A_3, \quad (18)$$

where $\gamma_1 = \gamma(k_1)$ represents both the effect of viscous dissipation and wind input. For $\gamma$, we take an expression proposed by Plant & Wright (1977),

$$\gamma(k) = k^2\left(\frac{\delta u_*^2}{\omega} - 2\nu_{\mathrm{w}}\right), \quad (19)$$

where $\nu_{\mathrm{w}}$ is the kinematic viscosity of water, $u_*$ is the friction velocity of the air flow and $\delta \approx 0.1/2\pi$. The first term represents the effect of wind input and the second term represents viscous dissipation. The growth rate $\gamma$ as a function of wavenumber $k$ is plotted in figure 1 for $u_* = 17$ cm/s and 21 cm/s. Clearly, the growth rate is a very sensitive function of $u_*$. This follows, for example, from the condition of zero growth rate, i.e. $\omega = \delta u_*^2/2\nu_{\mathrm{w}}$). Since for these high frequencies the effect of gravity may be neglected, one finds that the growth rate becomes zero for the wavenumber

$$k = u_*^{\frac{4}{3}}\left(\frac{T^{-\frac{1}{3}}\delta}{2\nu_{\mathrm{w}}}\right)^{\frac{3}{2}}.$$

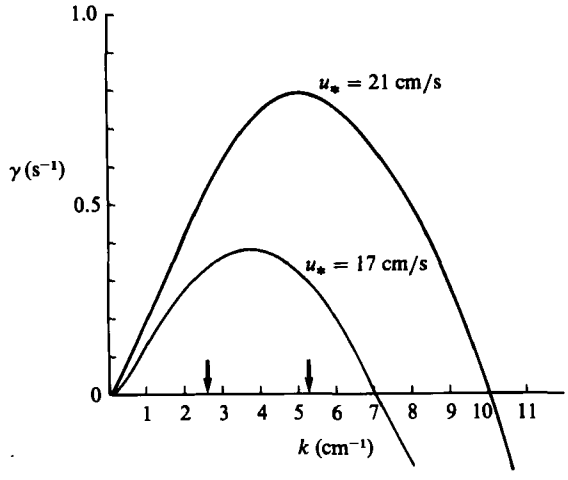


FIGURE 1. The growth rate $\gamma$ for gravity–capillary waves as a function of wavenumber for a friction velocity of 17 and 21 cm/s. Here, $\delta = 0.1/2\pi$, $\nu_w = 0.0114$, $g = 981$, $T = 74$.

Following a similar reasoning one finds that the maximum of the growth rate scales like $\gamma_{max} \sim u_*^{8/3}$. The modelling of all wind-induced and viscous effects by (19) is fairly crude. This model is however partly supported by observations and roughly in accord with numerical work of Kawai (1979) and theoretical estimates of Gastel, Janssen & Komen (1985). It is probably reasonably accurate for fairly short waves of small slope but certainly not for long waves that travel faster than the wind speed at 10 m, as (19) does not give a long-wave cutoff for instability.

## 3. Numerical treatment of wave–wave interactions

Before the numerical method to solve (18) is briefly discussed, we introduce dimensionless variables according to

$$\left.\begin{aligned} t' &= \frac{g^{\frac{3}{4}}}{T^{\frac{1}{4}}}t, \quad k' = k\left(\frac{T}{g}\right)^{\frac{1}{2}}, \quad \omega' = \frac{T^{\frac{1}{4}}}{g^{\frac{3}{4}}}\omega, \\ V' &= T^{\frac{7}{8}}g^{-\frac{9}{8}}V, \quad A' = g^{\frac{7}{8}}T^{-\frac{9}{8}}A. \end{aligned}\right\} \tag{20}$$

Then, the growth rate $\gamma$ transforms to

$$\gamma' = k'^2\left(\frac{\delta u'_*}{\omega'} - 2\nu'_w\right), \tag{21}$$

where

$$u'_* = u_*/(gT)^{\frac{1}{4}}, \; \nu'_w = \nu_w g^{\frac{1}{4}}/T^{\frac{3}{4}}$$

and

$$\omega' = (k' + k'^3)^{\frac{1}{2}}, \tag{22}$$

and the evolution equation becomes, dropping the primes from now on,

$$\frac{\partial}{\partial t}A_1 = (-\mathrm{i}\omega_1 s_1 + \gamma_1)A_1 - \mathrm{i}s_1 \int_{-\infty}^{\infty} \mathrm{d}\boldsymbol{k}_2 \mathrm{d}\boldsymbol{k}_3 \, \delta(\boldsymbol{k}_2 + \boldsymbol{k}_3 - \boldsymbol{k}_1) V(-1, 2, 3) A_2 A_3. \tag{23}$$

This equation will be solved for a finite number of modes. To that end the wave amplitude is represented as a finite series of Dirac delta functions,

$$A_1 = \sum_{j=-N}^{N} a_j \delta(k_1 - \Delta j),$$

where $\Delta$ is the spacing in wavenumber space. The evolution equation for $a_j$ becomes

$$\frac{\partial}{\partial t} a_j = (-\mathrm{i} s_j \omega_j + \gamma_j) a_j - \mathrm{i} s_j \sum_{l=-N}^{N} V(-j, l, j-l)\, a_l a_{j-l}, \quad j = -N, N. \tag{24}$$

This set of $2N+1$ ordinary differential equations was solved by means of a standard integration method (a Runge–Kutta 4 method). The discrete counterparts of the conserved quantities $P$ and $H$ are

$$\left.\begin{aligned} P &= \sum_{j=0}^{N} j|a_j|^2, \\ H &= \sum_{j=0}^{N} \omega_j |a_j|^2 + \sum_{j=0}^{N} \sum_{l=0}^{j} V(-j, l, j-l)\{a_j^* a_l a_{j-l} + \text{c.c.}\}. \end{aligned}\right\} \tag{25}$$

An appropriate measure for the spectral energy density would perhaps be the Hamiltonian density

$$H_j = \frac{\omega_j |a_j|^2}{\Delta} + \frac{1}{\Delta} \sum_{l=0}^{j} V(-j, l, j-l)\{a_j^* a_l a_{j-l} + \text{c.c.}\};$$

as in the case of no dissipation and growth by wind $H = \Sigma H_j \Delta$ is conserved. In an experiment, however, it is customary to measure the surface-elevation spectrum. The relation between the Fourier transform of the surface elevation, $\eta(k)$ and the amplitude $A$ is given by

$$\eta = \frac{1}{\sqrt{2}} \frac{k^{\frac{1}{2}}}{\omega^{\frac{1}{2}}} A.$$

In a discrete representation, $\eta = \Sigma \eta_j \delta(k - \Delta j)$, one therefore finds

$$\frac{1}{(2\pi)^2} \sum_{j=-N}^{N} |\eta_j|^2 = \langle \eta^2 \rangle, \tag{26}$$

where $\langle \eta^2 \rangle$ is the spatial average of the variance $\eta^2$,

$$\langle \eta^2 \rangle = \frac{1}{2L} \int_{-L}^{L} \mathrm{d}x\, \eta^2(x), \quad L = \frac{\pi}{\Delta}. \tag{27}$$

The surface-elevation spectrum $F_\eta$ is then defined as

$$F_\eta = 2 \frac{|\eta_j|^2}{(2\pi)^2 \Delta} = \frac{k}{\omega} \frac{|a_j|^2}{(2\pi)^2 \Delta}, \quad j = 0, N, \tag{28}$$

and the relation between dimensional and dimensionless quantities is

$$\langle \eta^2 \rangle = \frac{T}{g} \langle \eta'^2 \rangle, \quad F_\eta = F'_{\eta'} \left(\frac{T}{g}\right)^{\frac{3}{2}}. \tag{29}$$

Before we discuss in detail the evolution of the surface-elevation spectrum under generating conditions we consider some special examples. In order to check the numerical code we choose $N = 2$, $\Delta = 1/\sqrt{2}$ as this corresponds to the case of second-harmonic resonance, which may be solved exactly.

From (24) one has for $N = 2$

$$\left.\begin{aligned}\frac{\partial}{\partial t}a_1 &= (-\mathrm{i}\omega_1+\gamma_1)\,a_1-2\mathrm{i}Va_1^*a_2\\ \frac{\partial}{\partial t}a_2 &= (-\mathrm{i}\omega_2+\gamma_2)\,a_2-\mathrm{i}Va_1^2,\end{aligned}\right\} \tag{30}$$

where

$$V = V(-1,-1,2) = \frac{\Delta^{\frac{3}{4}}}{4\pi}(\tfrac{1}{2}\omega_1)^{\frac{1}{2}},$$

using the conditions for second-harmonic resonance, i.e. $\omega_2 = 2\omega_1$ and $k_2 = 2k_1$.

For $\gamma = 0$, (30) may be solved exactly in terms of elliptic functions as it has two conserved quantities. These immediately follow from (25) for $N = 2$, i.e.

$$P = \sum_{j=0}^{2} j|a_j|^2,$$

$$H = \omega_1 P + V(-1,-1,2)\{a_2^*a_1^2+\text{c.c.}\}.$$

Please note that as $P$ and $H$ are conserved, the conservation of $L = a_2^*a_1^2+\text{c.c.}$ follows at once. The latter conserved quantity is the one usually encountered in connection with second-harmonic resonance (McGoldrick 1972). The results of the numerical computation for the initial conditions $a_1(0) = 0.1$, $a_2(0) = 1$ are given in figure 1. In agreement with the analysis, periodic solutions are found with a maximum in the amplitude $a_1$ of 1.4175, whereas analytically one finds 1.4142. Wave momentum and energy are conserved to 6 significant digits.

In a second experiment we took a constant growth rate $\gamma = \gamma_1 = \gamma_2$. This case may also be solved exactly as the transformations

$$a_1 = \bar{a}_1\,\mathrm{e}^{\gamma t}, \quad a_2 = \bar{a}_2\,\mathrm{e}^{\gamma t}$$

and the introduction of a new timescale $\tau$,

$$\tau = \frac{\mathrm{e}^{\gamma t}-1}{\gamma},$$

just give the conservative equations for $\bar{a}_1(\tau)$, $\bar{a}_2(\tau)$. Clearly, when $\gamma$ is positive the interplay between the first and second harmonic occurs on a shorter timescale. We have illustrated this for the same initial conditions as the conservative case, with a growth rate $\gamma = 0.016$ (figure 3).

Janssen (1986) showed, using linear stability analysis, that this sudden transfer of energy from the second to first harmonic is also found for $\gamma_1 \neq \gamma_2$. He also studied the case that the resonance between the two modes is not perfect (because of a slight wavenumber mismatch, for example) and found no energy transfer from the second to first harmonic unless the wave amplitude of the second harmonic exceeded a certain value that depends on the wavenumber mismatch (see also Chen & Saffman 1979). If $h$ is the wave height of the wave at wavenumber $k$ the threshold condition is given by

$$h > \frac{2}{3k}\,|k^2-2| \tag{31}$$

and this condition holds true for $k^2 \approx 2$ and in the absence of wind.

The picture that emerges from these simple examples in clear. If the growth rate due to wind has a maximum around the second-harmonic wavenumber $k_0 = \sqrt{2}$ then

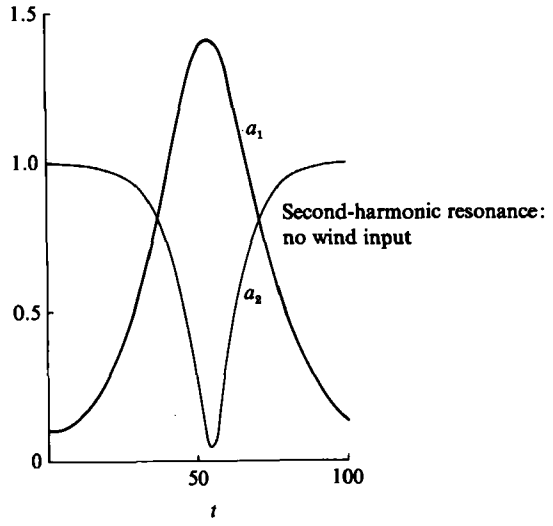


FIGURE 2. Absolute value of the amplitudes of the first and second harmonic, $a_1$ and $a_2$, respectively, as a function of time (no wind input).

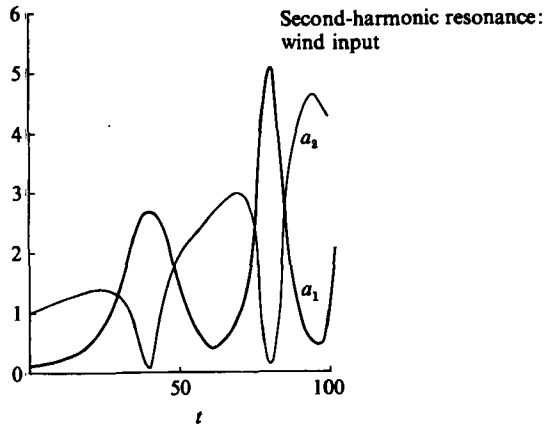


FIGURE 3. Absolute value of the amplitudes of the first and second harmonic, $a_1$ and $a_2$, respectively, as a function of time. Second-harmonic resonance with wind input. Note that the energy transfer occurs on a shorter timescale compared with figure 2.

the second harmonic will be generated first. This continues to happen until the wave height exceeds the threshold (31), then, depending on the position of the maximum of the wind input there will be a gradual or a sudden shift of the peak of the spectrum. If this maximum is close to $k_0$, condition (31) will be satisfied quite soon giving a rather gradual shift. If, however, the maximum is far from $k_0$ it takes a long time before the transfer condition (31) is satisfied. But, when (31) is satisfied, the amplitudes of the first and second harmonic have become considerable so that now a sudden transfer of energy from the second to first harmonic occurs. The question is, however, what will happen if many waves are allowed to evolve because the dispersion relation of the gravity–capillary admits other three-wave interactions as well? We will discuss this problem in §4.

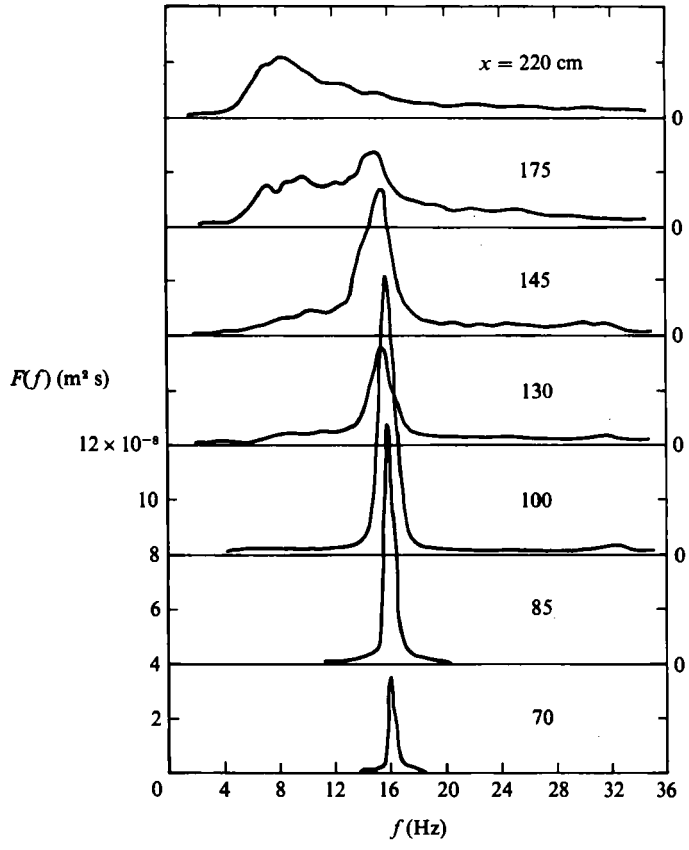


FIGURE 4. Evolution of frequency spectrum as a function of fetch (from Choi 1977).

## 4. Numerical simulation of wind-wave tank experiments

In this Section some numerical simulations of wind-generated surface waves in a wind-wave tank are described. We concentrate on Choi's (1977) experiment and briefly comment on the experiments of Kawai (1979). Choi investigated the generation of gravity–capillary waves by wind in the $\frac{1}{5}$-scale wind tunnel described by Favre & Coantic (1974). For a brief account of these results see also Ramamonjiarisoa, Baldy & Choi (1978).

For a wind speed of 5 m/s this experiment clearly revealed the period-doubling phenomenon, discussed in some detail by Janssen (1986). This is illustrated in figure 4 where the frequency spectrum for the surface elevation is given for different fetch. Another remarkable feature of figure 4 is that the spectrum at a fetch of 70 cm is narrower than is to be expected from the linear theory of wind-wave generation alone. The reason is that the maximum in the growth curve (see figure 1) is too broad. Assuming that the linear theory of wind-wave generation is correct this means that nonlinear effects must be responsible for the narrowing of the peak. We shall discuss this further when describing the numerical-simulation results.

We have solved the evolution equation (24) for $a_j$ for 50 modes. The constants for wind input and dissipation were chosen (in c.g.s. units) as $g = 981$, $T = 74$, $\nu_w = 0.0114$, $\delta = 0.1/2\pi$. The wavenumber is given by $k_j = \Delta_j$ and we have chosen

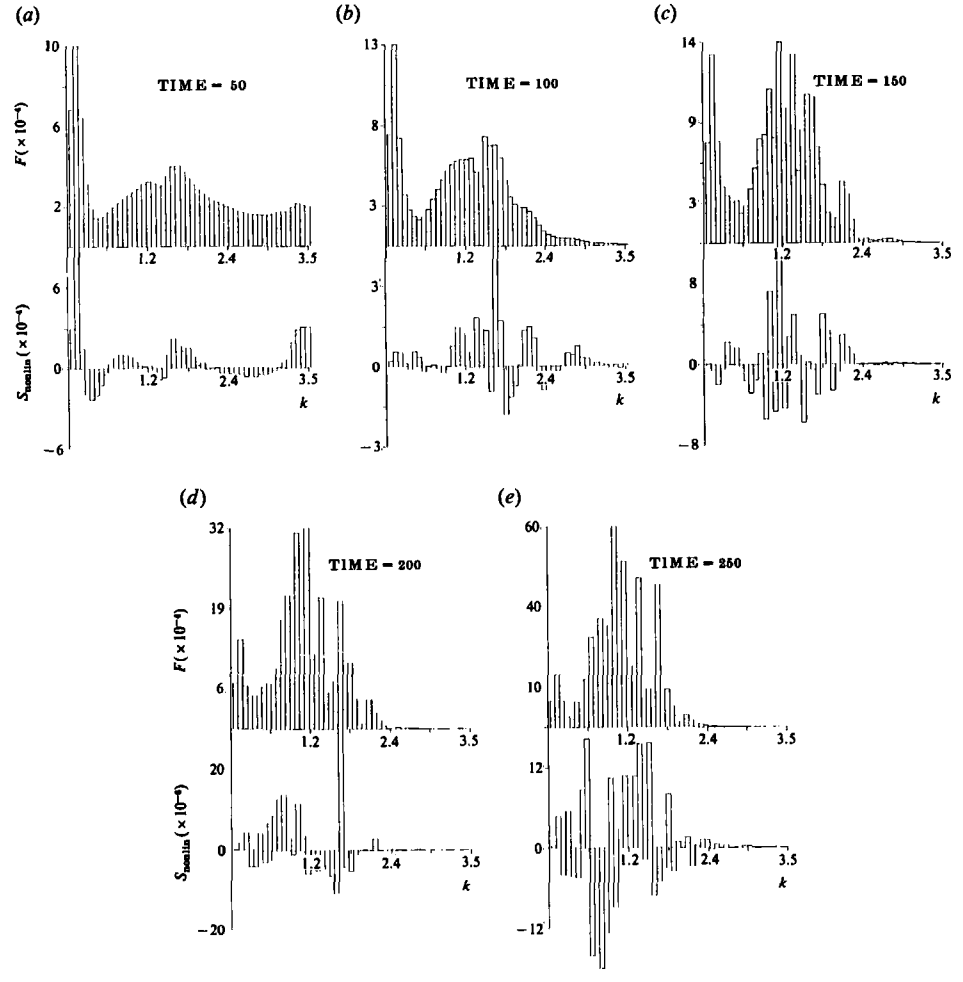


FIGURE 5. Evolution in time of the averaged surface-elevation spectrum and the averaged nonlinear transfer for $u_* = 17$ cm/s. Note the change of scale in the course of time. Here, $N = 50$ and $\Delta = 0.1/\sqrt{2}$. (*a*) $T = 50$; (*b*) 100; (*c*) 150; (*d*) 200; (*e*) 250.

the mesh width $\Delta$ in such a way that the waves enjoying second-harmonic resonance are included, i.e.

$$\Delta = 0.1/\sqrt{2}; \tag{32}$$

thus, waves with $k = k_{20}$ $(= \sqrt{2})$ and $k = k_{10}$ $(= \frac{1}{2}\sqrt{2})$ obey the conditions for second-harmonic resonance. The wave with wavenumber $k = k_{50}$ $(= 3.54)$ is heavily damped because of viscous dissipation. Therefore, the full inertial subrange and part of the viscous range is included in the simulation. This forced dissipative system with $N = 50$ is most likely to exhibit chaotic behaviour as shown before for the case of a three-wave interaction where one wave is growing owing to linear effects and the other two are heavily damped (cf. e.g. Russel & Ott 1981). Here, we concentrate on the downshift of the peak wavenumber, and shall consider aspects of chaotic behaviour, strange attractors etc. in a later study.

We shall discuss in some detail the results of numerical simulations at three different friction velocities, namely $u_* = 17, 21$ and 24 cm/s. The noise level was $\langle \eta^2(0) \rangle = 10^{-4} \times g/T$, in agreement with the level found in Choi's experiment.

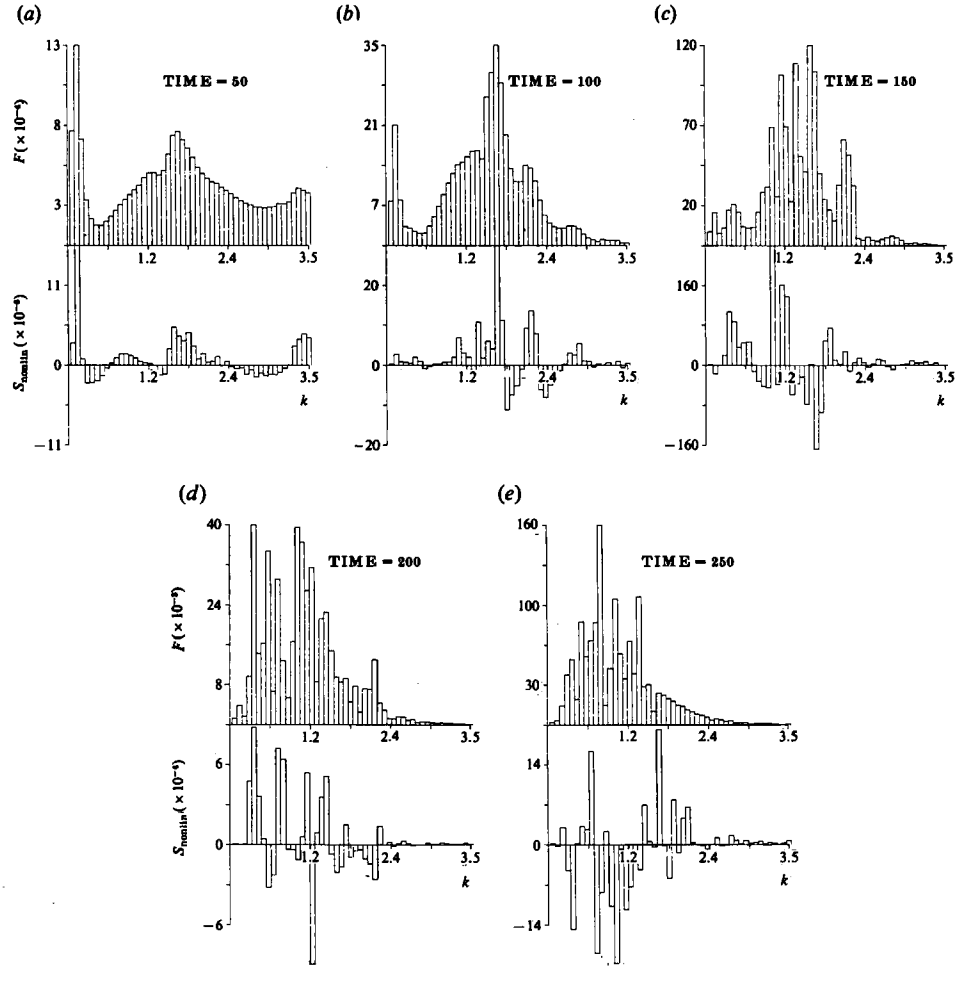


FIGURE 6. Evolution in time of the averaged surface elevation spectrum and the averaged nonlinear transfer for $u_* = 21$ cm/s. Note the change of scale in the course of time. Here $N = 50$ and $\Delta = 0.1/\sqrt{2}$. (*a*) $T = 50$; (*b*) 100; (*c*) 150; (*d*) 200; (*e*) 250.

In figures 5–7 we show the evolution in time of the surface-elevation spectrum $F_\eta$ (upper graph) and the rate of change of $F_\eta$ due to nonlinear interactions (S nonlin, lower graph) for, respectively, $u_* = 17$, 21 and 24 cm/s. The results shown are averaged over a time interval (cases $u_* = 17$ and 21 over a period of 50 units (i.e. about 1 s in real time) and the case $u_* = 24$ over a period of 25). These cases are discussed below.

*Case* $u_* = 17$ (*figure* 5)

Remarkably, nonlinear interactions are important from the start. This is seen at once from the fact that the linear growth is maximum for a wavenumber $k = k_{15}$ ($= 1.06$) whereas at $T = 50$ the peak of the spectrum is at $k = 1.63$. Also, at $T = 50$ and 100 much energy is being pumped into the low wavenumbers (these high energy levels are also seen in the spectra of Kawai 1979). The timescale $\tau_{\mathrm{NL}}$ for nonlinear interactions may be estimated; it is typically of the order $\tau_{\mathrm{NL}} \approx 150$, and is somewhat smaller than the timescale $\tau_{\mathrm{wind}}$ for linear growth ($\tau_{\mathrm{wind}} \approx 80$).

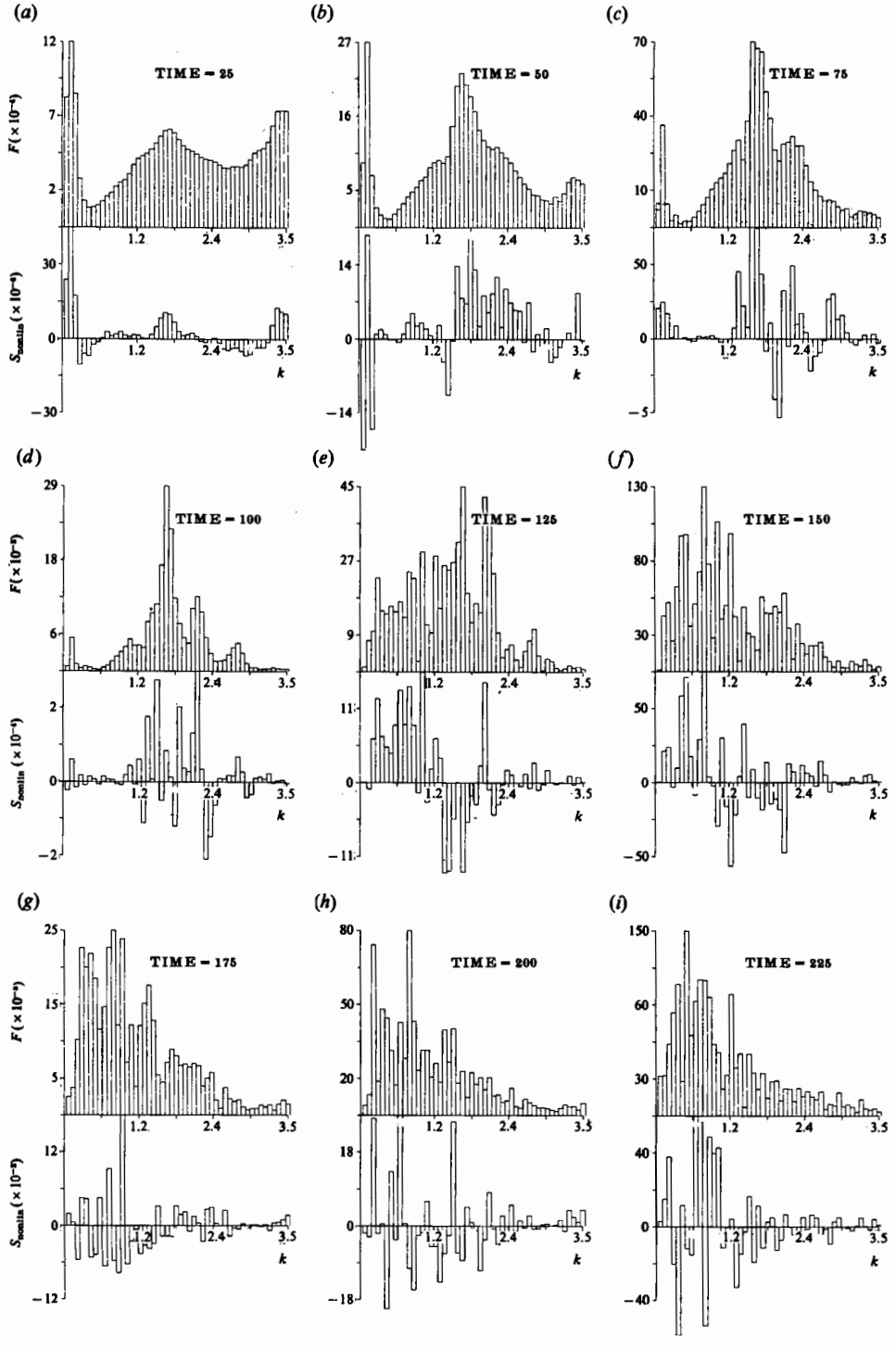


FIGURE 7. Evolution in time of the averaged surface-elevation spectrum and the averaged nonlinear transfer for $u_* = 24$ cm/s. Here, $N = 50$ and $\Delta = 0.1/\sqrt{2}$. (*a*) $T = 25$; (*b*) 50; (*c*) 75; (*d*) 100; (*e*) 125; (*f*) 150; (*g*) 175; (*h*) 200; (*i*) 225.

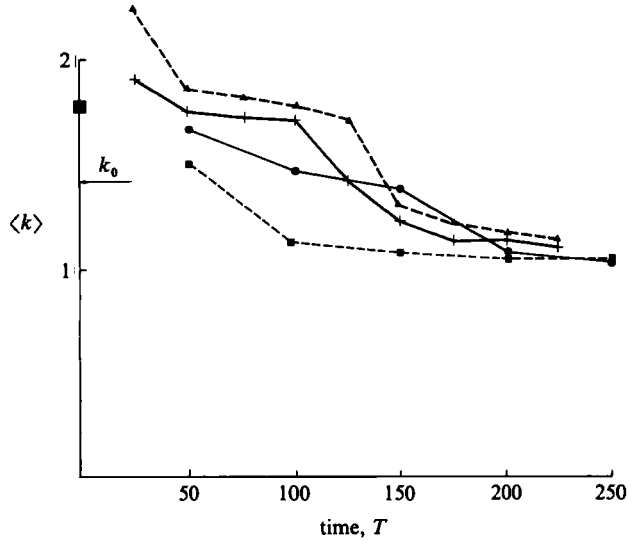


FIGURE 8. The average wavenumber $\langle k \rangle$ as a function of time $T$. Here, $N = 50$ and for $\alpha = 0.1/\sqrt{2}$ we have the cases ■, $u_* = 17$ cm/s; ●, $u_* = 21$ cm/s; +, $u_* = 24$ cm/s. Finally for $\alpha = 0.15/\sqrt{2}$ we show the case $u_* = 24$ cm/s (▲).

From $T = 100$, a slow migration of the peak towards lower wavenumbers may be observed. At $T = 250$ (this corresponds to about 5 s real time) the peak of the spectrum is at the wavenumber of maximum wind input.

We show the slow migration of the peak wavenumber in figure 8, where the averaged wavenumber, defined as

$$\langle k \rangle = \frac{\sum k_j F_\eta(j)}{\sum F_\eta(j)}. \tag{33}$$

is plotted as a function of dimensionless time $T$. No dramatic changes in the position of the peak of the spectrum were found in this simulation.

*Case* $u_* = 21$ (*figure* 6)

Again, nonlinear interactions are important from the start. A typical nonlinear timescale is $\tau_{\mathrm{NL}} \approx 70$, while $\tau_{\mathrm{wind}} \approx 40$. And again, at $T = 50$ the peak of the spectrum (at $k = 1.63$) is found at a slightly higher wavenumber than that of maximum growth rate (at $k = 1.41$). According to our plot of the average wavenumber $\langle k \rangle$ as a function of time $T$, there is a continuous migration of the peak wavenumber. Evidently, from inspection of the lower panels of figure 6, this slow migration is caused by the three-wave interactions.

*Case* $u_* = 24$ (*figure* 7)

The maximum of the growth rate for this case is at $k = k_{23} \approx 1.63$. During the initial stage (up to $T = 100$) a very narrow spectral peak is generated at $k = k_{23}$. According to the lower panel of figure 7 three-wave interactions tend to make the spectral peak narrower. In addition, during the initial stages the growth rate of the spectral peak is enhanced by as much as 50% owing to these three-wave interactions.

Thus, up to time $T = 100$ a narrow spectral peak is generated with a peak wavenumber slightly above that for second-harmonic resonance (this last wave-

number is at $k = k_{20} = 1.41$). At $T = 125$ a rather sudden migration of the peak, caused by three-wave interactions (cf. the lower panels of figure 7), occurs. This migration stops at around $T = 175$. Evidence for the sudden down shift in the spectral peak may also be found in the graph of the average wavenumber as a function of time $T$ (cf. figure 8).

One might wonder whether the results are sensitive to our choice of the wavenumber mesh width $\Delta$. We therefore performed one experiment for $u_* = 24$ cm/s with a larger mesh width

$$\Delta = 0.15/\sqrt{2}, \tag{34}$$

keeping the number of modes $N$ fixed ($N = 50$). The initial noise level was again $\langle \eta^2(0) \rangle = 10^{-4} * g/T$, hence the initial surface-elevation spectrum was smaller by a factor of two compared with our earlier experiments. Only during the initial stage is a significant departure from our earlier experiment found. The reason is that in this experiment also the high-wavenumber waves ($3.5 < k < 5.3$) have energy that is very efficiently dissipated by the effect of viscosity. The result is that, compared to the former simulation, this experiment has a somewhat delayed downshift of the peak. This is illustrated in figure 8 where we have plotted the averaged wavenumber as a function of time. Also note the large departure of $\langle k \rangle$ initially because of the 50% larger value of $\langle k(0) \rangle$. However, a different choice of mesh width and viscous subrange has no major effect on the downshift of the peak wavenumber.

We summarize the results of the numerical simulations as follows. In all cases second-harmonic resonance plays an important role in the evolution of the surface-elevation spectrum. This is also found in the initial stage as is illustrated most clearly by the case $u_* = 17$ cm/s where the maximum of the wind input is at wavenumber $k = k_{15}$, whereas at time $T = 50$ the maximum of the spectrum is at $k = k_{23}$. As a result, a rather broad spectrum is found at later times giving a gradual decrease of the average wavenumber. On the other hand, for the larger wind speed $u_* = 24$ cm/s the maximum of the wind input and an extremum of the nonlinear transfer coincides, resulting in a narrow spectrum at time $T = 100$ with a peak wavenumber just above the second-harmonic wavenumber, i.e. $k_{\text{peak}} = k_{23} = 1.63$, whereas the second-harmonic wavenumber is at $k = k_{20} = 1.41$. Inserting the peak wavenumber into the threshold condition (31) one finds that transfer of energy from the second to first harmonic starts to happen for a waveheight $h > 0.264$ which corresponds to a variance $\langle \eta^2 \rangle = \frac{1}{8}h^2 > 0.00874$. Now, the waveheight considered in the simple theory of §3 only refers to the waves around the second-harmonic peak. Estimating the variance of the peak of the spectrum by summing the surface-elevation spectrum of figure 7 at time $T = 100$ over the wavenumber range $k_{19} < k < k_{28}$, we find $\langle \eta^2 \rangle_{\text{peak}} \approx 0.009$. Based on the simple second-harmonic resonance theory of §3 one would therefore expect a considerable transfer of energy from the second to the first harmonic after time $T = 100$. This is clearly observed in the panels following $T = 100$ of figure 7.

We would like to remark here that there is qualitative agreement between our numerical simulations and the experiments of Choi (1977) and Kawai (1979). Quantitative agreement is however hardly to be expected as a number of physical effects are not included in our model, for example the effect of the water current induced by the wind and the shear in the water current. This not only affects the dispersion relation of the waves but also shear in the current will affect the interaction matrix $V$ and the resonance condition (Janssen 1986). Shear in the air flow might change $V$ as well giving a complex matrix instead of a real one (cf. Craik

1985), and therefore the nonlinear interactions are not conservative anymore. Incidentally, it should be noted that the effect of quadratic nonlinearity in the air is not as large for the surface waves as found for waves in a shear flow without a density gradient (see e.g. Craik 1985, p. 164). Although the first and second harmonic also have a common critical layer, the air density $\rho_a$ is much smaller than the water density $\rho_w$ so that the effect of shear in the air flow on the matrix $V$ will be

$$O\left(\frac{\rho_a}{\rho_w} Re\right),$$

where $Re = u_*/k\nu_a$, and $\nu_a$ is the kinematic viscosity of air. Hence, as $\rho_a/\rho_w \approx 0.001$ and, for the experimental conditions of interest, $Re \approx 100$ the effect of shear in the air flow might still be small.

We have only performed integrations with this model for one-dimensional propagation. The spanwise variation of the wave field will be included in future work, as two-dimensional effects are believed to be important. For example, Kawai (1979) shows photographs of the water surface with strong spanwise variations.

## 5. Conclusions

We have discussed a numerical model of the evolution of wind-generated, gravity–capillary waves. This model includes the effects of energy input by wind, energy dissipation by viscosity and energy redistribution among the waves by nonlinear three-wave interactions.

A rather sudden migration of the peak of the spectrum is observed provided the peak wavenumber is larger than the wavenumber $k_0$ for second-harmonic resonance and provided the waveheight corresponding to this peak is sufficiently large. There is qualitative agreement with results obtained from a simple model of second-harmonic resonance (Janssen 1986) and with wave-tank experiments of Choi (1977) and Kawai (1979). In particular, it was also shown that in the presence of many waves second-harmonic resonance plays an important role in the evolution of gravity–capillary waves.

Remarkably, even in the stage of the initial wavelets (a term introduced by Kawai 1979) the effect of nonlinear three-wave interactions may be comparable with the effect of wind. There is no need to emphasize then that the determination of the growth rate of the waves by wind through an analysis of the time series of the surface elevation of the waves might be in error by a factor of two. Therefore, according to our results, an alternative technique for the determination of energy transfer from the wind to the gravity–capillary waves has to be found. Incidentally, an analogy may be drawn between the present status of research in gravity–capillary waves and the status of understanding of long, surface gravity waves by the end of the sixties when the important role of four-wave interactions on the behaviour of these long waves was realised.

Finally, it is noted that our results have been derived from deterministic evolution equations. The use of statistical evolution equations would be perhaps more desirable, if only because less computation time is needed. (A typical run with the deterministic equations took 15 min c.p.u. time on a Cray-XMP-48.) However, a reconsideration of the conventional statistical theory for the case of second-harmonic resonance is then needed since the relation (6) was certainly not satisfied in our simulations.

The author is please to acknowledge numerous discussions with Gerbrand J. Komen. The computations were performed on the Cray XMP-48 of the European Centre for Medium Range Weather Forecasts in Reading, England.

## REFERENCES

BROER, L. J. F. 1974 *Appl. Sci. Res.* **30**, 430–446.

CHEN, B. & SAFFMAN, P. G. 1979 Steady gravity–capillary waves in deep water – I. Weakly nonlinear waves. *Stud. Appl. Maths* **60**, 183–210.

CHOI, I. 1977 Contributions a l'étude des mechanismes physiques de la génération des ondes de capillarité–gravité à une interface air-eau. Thesis, Université d'Aix Marseille.

CRAIK, A. D. D. 1985 *Wave Interactions and Fluid Flows*. Cambridge University Press.

CRAWFORD, D. R., LAKE, B. M., SAFFMAN, P. G. & YUEN, H. C. 1981 Effects of nonlinearity and spectral bandwidth on the dispersion relation and component phase speeds of surface gravity waves. *J. Fluid Mech.* **112**, 1–32.

DAVIDSON, R. C. 1972 *Methods in Nonlinear Plasma Theory*. Academic.

FAVRE, A. & COANTIC, M. 1974 Activities in the preliminary results of air–sea interaction at IMST. *Adv. Geophys.* **10A**, 291–405.

GASTEL, K. VAN, JANSSEN, P. A. E. M. & KOMEN, G. J. 1985 On phase velocity and growth rate of wind-induced gravity–capillary waves. *J. Fluid Mech.* **161**, 199–216.

JANSSEN, P. A. E. M. 1986 The period doubing of gravity–capillary waves. *J. Fluid Mech.* **172**, 531–546.

KAWAI, S. 1979 Generation of initial wavelets by instability of a coupled shear flow and their evolution to wind waves. *J. Fluid Mech.* **93**, 661–703.

MCGOLDRICK, L. F. 1972 On the rippling of small waves: a harmonic nonlinear resonant interaction. *J. Fluid Mech.* **52**, 725–751.

MILES, J. W. 1977 On Hamilton's principle for surface waves. *J. Fluid Mech.* **83**, 153–158.

PLANT, W. J. & WRIGHT, J. W. 1977 Growth and equilibrium of short gravity waves in a wind-wave tank. *J. Fluid Mech.* **82**, 767–793.

RAMAMONJIARISOA, A., BALDY, S. & CHOI, I. 1978 Laboratory studies on wind-wave generation, amplification and evolution. In *Turbulent Fluxes through the Sea Surface, Wave Dynamics, and Prediction* (ed. A. Favre & K. Hasselmann), pp. 403–420. Plenum.

RUSSEL, D. A. & OTT, E. 1981 Chaotic (strange) and periodic behaviour in instability saturation by the oscillation two-stream instability. *Phys. Fluids* **24**, 1976–1988.

SIMMONS, W. F. 1969 A variational method for weak resonant wave interactions. *Proc. R. Soc. Lond.* A **309**, 551–575.

VALENZUELA, G. R. & LAING, M. B. 1972 Nonlinear energy transfer in gravity–capillary wave spectra, with applications. *J. Fluid Mech.* **54**, 507–520.

ZAKHAROV, V. E. 1968 Stability of periodic waves of finite amplitude on the surface of a deep fluid. *Zh. Prikl. Mekh. Tekh. Fiz.* **2**, 86–94 (Translated in *J. Appl. Mech. Tech. Phys.* **2**, 190–194).